Supporting Information

In Vitro Evaluation of the Conjugations of Neonicotinoids with Transport Protein: Photochemistry, Ligand Docking and Molecular Dynamics Studies

Wei Peng,[abc] Fei Ding*[ad] and Yu-Kui Peng[e]

[a] *College of Agriculture and Plant Protection, Qingdao Agricultural University, Qingdao 266109, China*

[b] *College of Food Science and Engineering, Qingdao Agricultural University, Qingdao 266109, China*

[c] *Department of Chemistry, China Agricultural University, Beijing 100193, China*

[d] *Department of Biological Engineering, Massachusetts Institute of Technology, Cambridge, MA 02139, United States*

[e] *Center for Food Quality Supervision & Testing, Ministry of Agriculture, College of Food Science & Engineering, Northwest A&F University, Yangling 712100, China*

*Corresponding Author
Phone/fax: +86-29-87092367
E-mail: alexf.ting@outlook.com, feiding@cau.edu.cn

Time-resolved Fluorescence. Time-resolved fluorescence was examined with a FLS920 spectrometer (Edinburgh Instruments, UK), using the time-correlated single photon counting system with a hydrogen flash lamp excitation source, in air equilibrated solution at an ambient temperature. The excitation wavelength was 295 nm and the number of counts gathered in the channel of maximum intensity was 4,000. The instrument response function (IRF) was gauged exploiting Ludox to scatter light at the excitation wavelength. The data were analyzed with a nonlinear least-squares iterative method utilizing the Fluorescence Analysis Software Technology, which is a sophisticated software package designed by Edinburgh Photonics for the analysis of fluorescence and phosphorescence decay kinetics, IRF was deconvoluted from the experimental data, and the resolution limit after deconvolution was 0.2 ns. The value of χ^2 (0.9～1.2), the Durbin-Watson parameter (greater than 1.7), as well as a visual inspection of the residuals were used to assess how well the calculated decay fit the data. Average fluorescence lifetime (τ) for multiexponential function fittings were from the following relation:[1,2]

$$I(t) = \sum_i A_i e^{\frac{-t}{\tau_i}} \tag{1}$$

where τ_i are fluorescence lifetimes and A_i are their relative amplitudes, with i variable from 1 to 2.

Extrinsic ANS Displacement. In the first series of experiments, albumin concentration was kept fixed at 1.0 μM, and imidacloprid/ANS concentration was varied from 2.0 to 18 μM, albumin fluorescence was gained (λ_{ex}＝295 nm, λ_{em}＝338 nm). In the second series of experiments, imidacloprid was added to solutions of albumin and ANS held in equimolar concentration (1.0 μM), and the concentration of imidacloprid was also varied from 2.0 to 18 μM, the fluorescence of ANS was recorded (λ_{ex}＝370 nm, λ_{em}＝465 nm).

Site-specific Ligand Binding. Binding location studies between albumin and imidacloprid in the presence of four classic site markers (warfarin, diazepam, digitoxin and hemin) were executed using the fluorescence titration approach. The concentration of albumin and site markers were held in equimolar (1.0 μM), then imidacloprid was added to the albumin-site markers mixtures. An excitation wavelength of 295 nm was chosen and the fluorescence emission wavelength was acquired from 300 to 500 nm.

CD Spectra. Far-UV CD spectra were collected with a Jasco-815 spectropolarimeter (Jasco, Japan) equipped with a microcomputer, the apparatus was sufficiently purged with 99.9% dry nitrogen gas before starting the instrument and then it was calibrate with d-10-camphorsulfonic acid. All the CD spectra were got at 298 K with a PFD-425S Peltier temperature controller attached to a water bath with an accuracy of $\pm$0.1 ^{o}C. Each spectrum was performed with use of a precision quartz cuvette of 1.0 cm path length and taken at wavelengths between 200 and 260 nm range that provides a signal extremely sensitive to small secondary conformational distortions. Every determination was the average of five successive scans encoded with 0.1 nm step resolution and recorded at a speed of 50 nm min^{-1} and response time of 1 s. All observed CD data were baseline subtracted for buffer and the estimation of the secondary structure elements was obtained by exploiting Jasco Spectra Manager II, which computes the different designations of secondary structures by comparison with CD spectra, determined from distinct proteins for which high-quality X-ray diffraction data are available.

Principles of Fluorescence Quenching. Fluorescence quenching refers to any process that decreases the fluorescence intensity of a sample. A variety of molecular interactions can result in quenching, such as excited state reactions, molecular rearrangements, energy transfer, ground state complex formation, and collisional quenching. Fluorescence quenching is described by the well-known Stern-Volmer equation:[1,3-5]

$$\frac{F_0}{F} = 1 + k_q \tau_0 [Q] = 1 + K_{SV} [Q] \quad (2)$$

In this equation, F_0 and F are the fluorescence intensities in the absence and presence of quencher, respectively, k_q is the bimolecular quenching constant, τ_0 is the lifetime of the fluorophore in the absence of quencher, [Q] is the concentration of quencher, and K_{sv} by linear regression of a plot of F_0/F *versus* [Q].

Evaluation of Association Ability. When ligand molecules bind independently to a set of equivalent sites on a macromolecule, the equilibrium between free and bound ligand molecules is given by the following relation:[6-9]

$$\log\frac{F_0 - F}{F} = \log K + n\log[Q] \tag{3}$$

In this equation, F_0 and F are the fluorescence intensities in the absence and presence of quencher, respectively, K and n are the association constant and the number of binding sites, respectively, [Q] is the concentration of quencher. Thus, a plot of $\log(F_0 - F)/F$ *against* $\log[Q]$ can be used to calculate K and n. Moreover, the fluorescence intensities were corrected for absorption of the exciting light and reabsorption of the emitted light to decrease the inner filter effect by using the following relationship:[1]

$$F_{cor} = F_{obs} \times e^{\frac{A_{ex} + A_{em}}{2}} \tag{4}$$

where F_{cor} and F_{obs} are the fluorescence intensities corrected and observed, respectively, and A_{ex} and A_{em} are the absorption of the systems at the excitation and the emission wavelength, respectively. The fluorescence intensity utilized in this work is the corrected intensity.

Ligand Binding Domain. As we have seen, the 1∶1 complexation is predominant at the protein-neonicotinoid equilibrium, and there is only one binding domain in protein for neonicotinoid. To ascertain the concrete functional cavity on protein for neonicotinoid compound, guanidine hydrochloride (GuHCl) evoked unfolding studies of protein were firstly performed in this section. Generally, there are several approaches to unfold a protein according to the damage of the noncovalent bonds, i.e. hydrogen bonds, hydrophobic interactions, π-π stacking and van der Waals interactions that keeps the protein folded, and the most common manners of unfolding a protein are chaotropic agents, e.g. GuHCl and urea. As Ahmad et al.[10] have stated, GuHCl induced albumin unfolding to take place in multiple steps, at 1.4 M GuHCl, only domain III is completely unfolded, the presence of a molten globule-like intermediate state of domain III is around 1.8 M GuHCl concentration and at 3.2 M GuHCl, domain I is departed from the domain II, domain I is fully unfolded while domain II is partly. This unfolding action has been affirmed by Galantini et al.,[11] who explored a small-angle X-ray scattering and light scattering techniques to illuminate the unfolding cartoon of fatted and defatted albumin. In the current circumstance, samples of different GuHCl were prepared by blending varied molar ratios of GuHCl stock solution and Tris-HCl buffer of pH＝7.4. The final solution mixture was incubated with various GuHCl concentrations for 12 h at room temperature before fluorescence emission determinations. Relative to the hydrophobic environment, the quantum yield of aromatic amino acid residues reduces leading to low fluorescence

intensity in a hydrophilic environment (exposed to solvent).[7] Particularly, there is forceful Stokes shift for Trp residue in albumin relies on the solvent, suggesting that the maximum fluorescence emission wavelength of Trp residue will diverge counting on the residue microenvironment (data not shown). Linear equation (3) was also used to fit the association constants in the existence of different concentrations of GuHCl, and the data (298 K) were found to be 1.212×10^4 M^{-1}, 0.9587×10^4 M^{-1} and 0.2344×10^4 M^{-1} at 1.4 M, 1.8 M and 3.2 M GuHCl, respectively. This result certifies that the unfolding of domain II clearly affects the neonicotinoid binding to albumin, or rather domain II of protein retain high-affinity site of this insecticide.

Ideally, 8-anilino-1-naphthalenesulfonic acid (ANS) is one of the most frequently used fluorescent chemicals for the examination of nonpolar sites in proteins, and previously in 1966 ANS fluorescence was efficaciously employed to characterize five hydrophobic domains on bovine serum albumin.[12] For the moment ANS is extensively utilized as a reporter of nonpolar surface pockets of proteins or as a back titration fluorescence indicator for lipid ligand displacement from lipid transporter proteins or, in general, analysis of protein structural features.[13,14] To further test the nature of the binding site of neonicotinoid in albumin, binding studies were conducted in the presence of ANS under the identical conditions, and the relative fluorescence intensity (F/F_0) *versus* ligand concentration ([Ligand]) plots is displayed in Fig. S4. At a ligand concentration of 18 μM, both neonicotinoid and ANS had quenching effect on albumin fluorescence, but the level was somewhat different; ANS could quench 75.74%, while neonicotinoid can only decrease 55.39% of Trp-214 residue

fluorescence. Stryer[15] first discovered that the quantum yield of free ANS in water is about 0.004 and becomes as high as 0.98 when the dye molecules are bound to apomyoglobin. And he has also set up that the fluorescence of ANS bound to the nonpolar sites of apomyoglobin and apohemoglobin was equal to the fluorescence of an equivalent mass of ANS in a number of hydrophobic organic solvents.[14,15] Therefore, when neonicotinoid is added to the ANS-albumin complex, it may contend for hydrophobic sites, and the fluorescence of ANS would weaken. It is plain from Fig. S4 that nearly 29.9% of ANS fluorescence faded in the presence of 18 μM neonicotinoid, hinting that neonicotinoid might compete against ANS for its binding region in protein. Although still partly controversial, consensus exists today that there are four hydrophobic binding sites for ANS associated with albumin, but preferentially at a site in subdomain IIIA.[16] Given the current situation, approximately 29.9% displacement of ANS fluorescence explains that neonicotinoid and ANS does not share a common site in albumin, in other words, neonicotinoid binds within subdomain IIA, Sudlow's site I. This conclusion is consistent with the induction based on denaturation of protein by GuHCl and also agrees well with the following site-specific competitive experiments using several classical ligands as designated site markers.

Fig. S4 here about

The aim of executing site-specific competitive experiments was to further substantiate the essence of the neonicotinoid binding pocket in albumin. As previously mentioned, albumin is known to include two well-defined binding sites,

called Sudlow's site I and site II, as well as several minor binding regions.[17-19] Site I is known as the warfarin-azapropazone site, and formed as a cavity in subdomain IIA, the lone Trp-214 residue of the albumin in this region. The inside wall of the pocket is comprised by hydrophobic side chains, while the entrance to the patch is surrounded by positively charged residues.[20,21] The curious feature of this site is the binding of the ligand, which is a bulky heterocyclic anion with a negative charge localized in the center of the molecule. Ligands binding in site I involve azapropazone, iodipamide, phenylbutazone and warfarin. Site II corresponds to the region of subdomain IIIA, and is known as the indole-benzodiazepine site, which is almost the same size as site I, the interior of the cavity is constituted by hydrophobic amino acid residues and the exterior domain presented two significant amino acid residues, i.e. Arg-410 and Tyr-411.[22,23] Drugs binding to site II are aromatic carboxylic acids with negatively charged acidic group at the end of the molecule, such as diazepam, flufenamic acid, halothane and ibuprofen. Subsequently, Brodersen et al.[24] pointed out that digitoxin binding in albumin is independent from Sudlow's nomenclature, and perch on what was nominated as site III. In the content, the competitors used included warfarin, a typical marker for site I, diazepam for site II, digitoxin for site III and hemin for domain I. According to equation (3), the association constants were fitted from fluorescence data and observed to be 0.2513×10^4 M^{-1}, 1.359×10^4 M^{-1}, 1.271×10^4 M^{-1} and 1.238×10^4 M^{-1}, respectively, for warfarin, diazepam, digitoxin and hemin. Evidently, the albumin-neonicotinoid adduct was most influenced by the addition of warfarin, i.e. neonicotinoid shares the same binding domain with warfarin in protein,

that is Sudlow's site I.

The Mutation of Phe-211 and Arg-222 Residues. Despite the mutation of Trp-214 residue, the residues Phe-211 and Arg-222 have also been mutated to alanine (Ala), respectively, and the results of mutated protein-neonicotinoid systems are shown in Fig. S5(A). Since the residue Phe-211 has been mutated to the nonaromatic and nonpolar Ala residue, some striking differences can be observed in the binding conformation of imidacloprid and the noncovalent interactions of the mutated protein-neonicotinoid complexes. For example, the oxygen atom of the polar nitryl and the nitrogen atom in the pyridine ring may only form two hydrogen bonds with the hydrogen atom of the amino group in Lys-199 and the hydrogen atom of the hydroxyl group in Ser-202 residues, and the bond lengths are 3.03 Å and 2.76 Å, respectively. Meanwhile, the conformational change in imidacloprid enticed the drop of originally strong conjugated effect between Trp-214 residue and neonicotinoid, and the distance is found to be 3.20 Å. These amino acid residues such as Ala-211, Trp-214, Ala-215, Leu-219 and Leu-238 stood around the neonicotinoid compound, but the hydrophobic interactions abated slightly owing to the displacement of imidacloprid conformation. Therefore, it can be seen that Phe-211 residue is one of the most important amino acid residues in the biointeractions of enzyme/protein with part neonicotinoid insecticides.

What transformations will be taken place in the recognition behavior of imidacloprid if the Arg-222 residue changes into Ala residue? To answer this question, some pertinent discussions about the binding mode have also been done in the current situation, and the result is displayed visibly in Fig. S5(B). There was little change in

the orientation of imidacloprid conformation, the nitrogen atom in pyridine ring can make hydrogen bond with the hydrogen atom of the hydroxyl group in Ser-202 residue, and the bond length is 2.82 Å. And the parallel distance between the center of the pyridine ring in imidacloprid and the core of the indole ring in Trp-214 residue is 3.37 Å, which indicated the existence of somewhat π-π interactions between them. However, the noncovalent forces of the overall adduct have obvious downhill trend compared with the native protein-neonicotinoid complex, probably this phenomenon springs from the fact that the polar nitryl in imidacloprid could not be able to produce hydrogen bonds with the ambient amino acid residues in the active pocket.

To verify the reasonableness and stableness of recognition pattern for the mutated protein-imidacloprid adducts, molecular dynamics (MD) simulation has been carried out in this section. Regarding the mutation of residue Phe-211 to Ala residue (Fig. S6(A)), the noncovalent interactions between mutated protein and imidacloprid are perceptibly tending downwards in the process of MD simulation. The plane of indole ring in Trp-214 residue has a tendency to approach the pyridine ring in imidacloprid, and π-π interactions have moderately increased in dynamic process, but the bond lengths hydrogen bonds between mutated protein and neonicotinoid imidacloprid are observed to be noticeably augmented at the same time. Moreover, the disappearance of hydrogen bond between the nitrogen atom in the pyridine ring and the hydrogen atom of the hydroxyl group in Ser-202 residue may be attributed to the torsion of the pyridine ring, and the spatial displacement of residue Lys-199 in MD simulation also revealed that Lys-199 residue hold the inclination to remote from the polar functional

nitryl in imidacloprid. Consequently, these points led to the depression of entire noncovalent forces in the conjugate. And this further indicates that the presence of Phe-211 residue has great influence on the molecular recognition of neonicotinoid by protein.

As regards the mutational behavior of residue Arg-222, the data of Root-Mean-Square Deviation (RMSD) validates the conformational stability of the mutated protein-imidacloprid reaction in MD simulation (Fig. 10). The average conformation in dynamic equilibrium suggests that the mutation of Arg-222 residue to Ala residue can actually give rise to arresting reduction of the association ability between protein and imidacloprid (Fig. S6(B)), even other neonicotinoid compounds. And the conjugated effect similar to the “sandwich” is found to be no longer existed in the mutated protein-imidacloprid and the shrinkage of hydrogen bonds are distinctly detected simultaneously, these aspects definitely led to the depreciation of the integral recognition affinity. Thereby we believe that the residue Arg-222 also acts a prominent role in the noncovalent protein-neonicotinoids reaction.

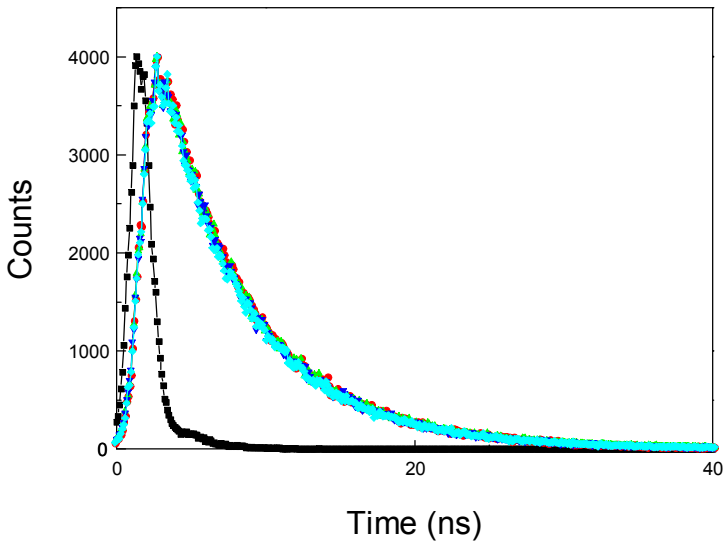

Fig. S1. Time-resolved fluorescence decays of albumin in Tris-HCl buffer (pH＝7.4) as a function of imidacloprid concentrations. *c*(albumin)＝10 μM, *c*(imidacloprid)＝0 (red), 10 (green), 20 (blue) and 40 (cyan) μM. The sharp pattern on the left (black) is the lamp profile.

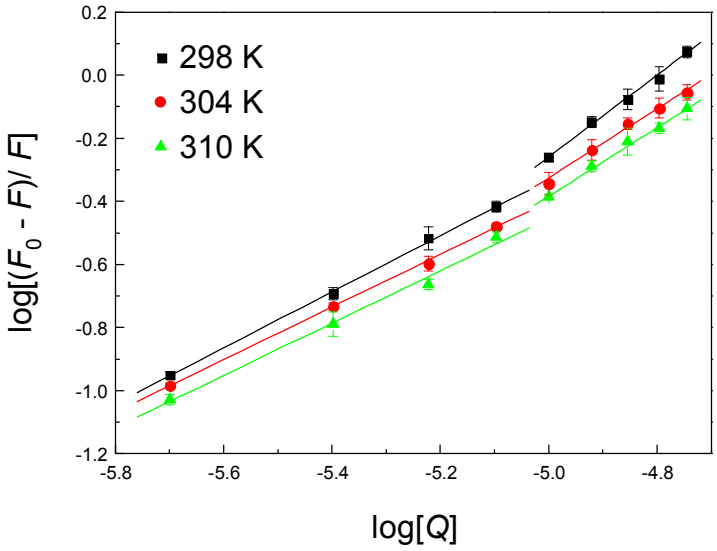

Fig. S2. Association constant plot presenting Trp-214 residue fluorescence quenching of albumin (1.0 μM) at pH＝7.4 induced by imidacloprid. The fluorescence intensity was recorded at λ_{ex}＝295 nm, and the λ_{em} maximum occurred at 338 nm. Each point was the mean of three individual experiments±S.D. ranging 0.89%～4.26%.

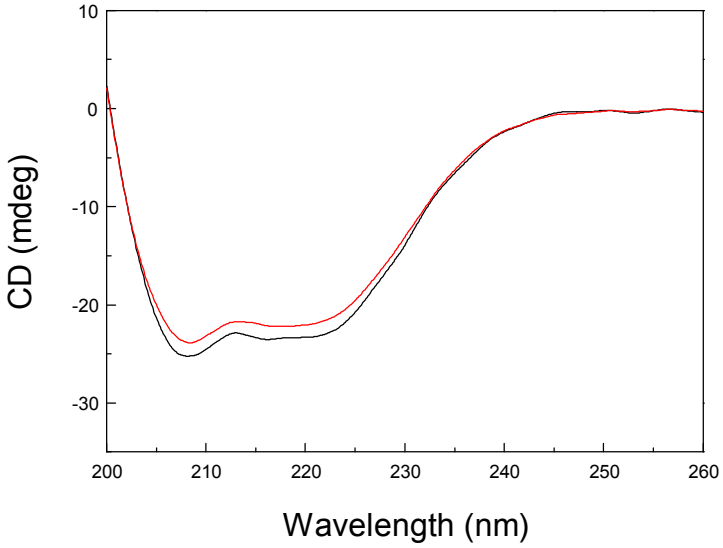

Fig. S3. Far-UV CD spectra of albumin complexes with imidacloprid (pH＝7.4, T＝298 K). (black): c(albumin)＝1.0 μM, c(imidacloprid)＝0; (red): c(albumin)＝1.0 μM, c(imidacloprid)＝8.0 μM.

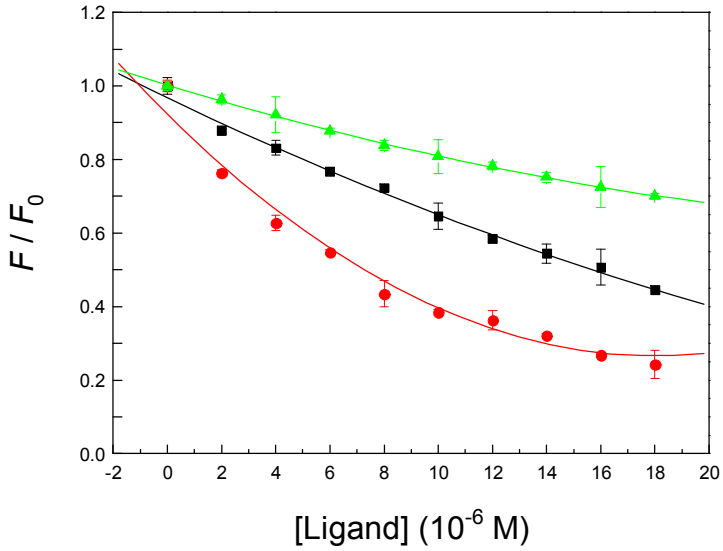

Fig. S4. Fluorescence quenching pictures of albumin and ANS-albumin adduct at pH＝7.4, *T*＝298 K. Binding isotherm of imidacloprid (■) and ANS (●) caused quenching of Trp-214 residue fluorescence and quenching of ANS-albumin complex fluorescence (▲) by imidacloprid. All data were corrected for imidacloprid fluorescence and each point was the average of three individual experiments±S.D. ranging 0.29%～5.59%.

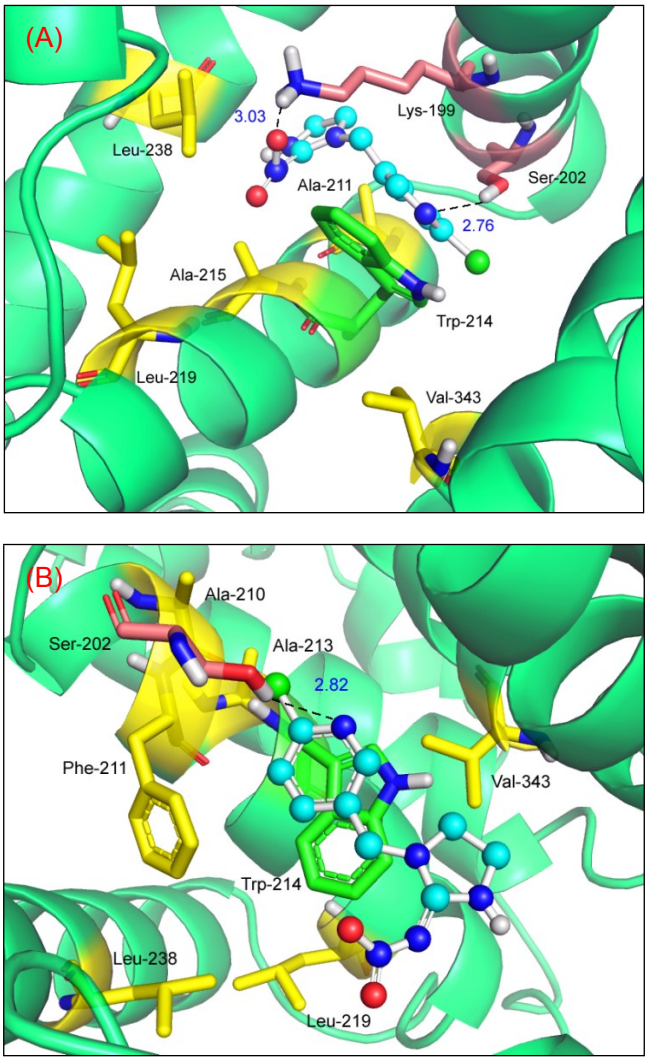

Fig. S5. Molecular modeling of imidacloprid docked to mutated albumin, (A): Phe-211→Ala, and (B): Arg-222→Ala residues, respectively. The ball-and-stick model shows imidacloprid, colored as per the atoms and key amino acid residues around imidacloprid have been displayed in stick model; salmon and yellow stick model indicates hydrogen bonds and hydrophobic interactions between mutated albumin and imidacloprid, respectively. (For interpretation of the references to color in this figure legend, the reader is referred to the web version of the article.)

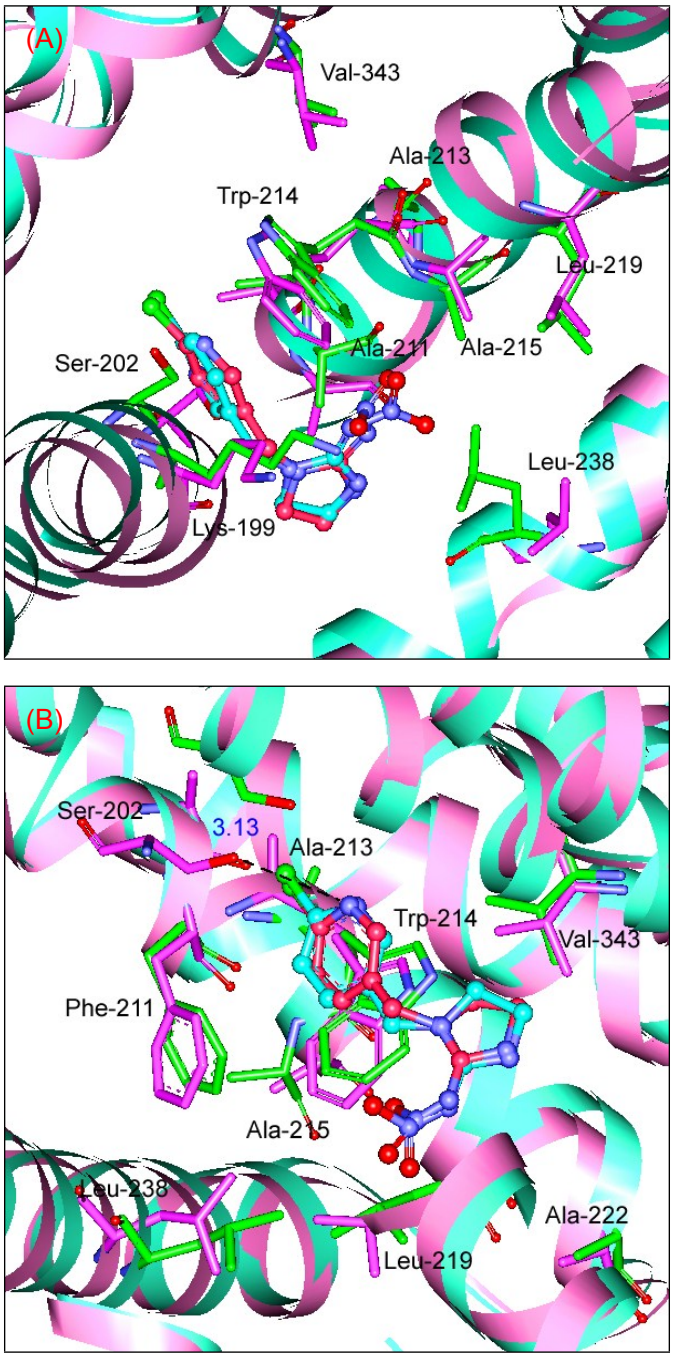

Fig. S6. Superposition of the mean conformation of MD simulation on the original conformation of molecular docking resulting from mutated albumin-imidacloprid complex, (A): Phe-211→Ala, and (B): Arg-222→Ala residues, respectively. Protein expounded in surface colored in blue green (initial) and pink (average), respectively, and the original and average conformations of imidacloprid annotated in cyan and hot pink ball-and-stick model. The green and pink stick model elucidates respectively the initial and average conformations of the pivotal amino acid residues involved in the

mutated albumin-imidacloprid reaction process. (For interpretation of the references to color in this figure legend, the reader is referred to the web version of the article.)

REFERENCES

1. J. R. Lakowicz, *Principles of Fluorescence Spectroscopy*, Springer Science+ Business Media, New York, NY, 3rd edn., 2006.
2. J. R. Albani, *Principles and Applications of Fluorescence Spectroscopy*, John Wiley & Sons, Inc., Hoboken, NJ, 2007.
3. B. Valeur, *Molecular Fluorescence: Principles and Applications*, John Wiley & Sons, Inc., Hoboken, NJ, 2007.
4. O. K. Abou-Zied, *Phys. Chem. Chem. Phys.*, 2012, **14**, 2832-2839.
5. B. P. Pahari, S. Chaudhuri, S. Chakraborty and P. K. Sengupta, *J. Phys. Chem. B*, 2015, **119**, 2533-2545.
6. O. K. Abou-Zied and O. I. K. Al-Shihi, *J. Am. Chem. Soc.*, 2008, **130**, 10793-10801.
7. O. K. Abou-Zied and N. Al-Lawatia, *ChemPhysChem*, 2011, **12**, 270-274.
8. D. P. Yeggoni and R. Subramanyam, *Mol. BioSyst.*, 2014, **10**, 3101-3110.
9. S. K. Chaturvedi, E. Ahmad, J. M. Khan, P. Alam, M. Ishtikhar and R. H. Khan, *Mol. BioSyst.*, 2015, **11**, 307-316.
10. B. Ahmad, M. Z. Ahmed, S. K. Haq and R. H. Khan, *Biochim. Biophys. Acta – Proteins Proteomics*, 2005, **1750**, 93-102.
11. L. Galantini, C. Leggio and N. V. Pavel, *J. Phys. Chem. B*, 2008, **112**, 15460-15469.

12. E. Daniel and G. Weber, *Biochemistry*, 1966, **5**, 1893-1900.

13. G. M. Edelman and W. O. McClure, *Acc. Chem. Res.*, 1968, **1**, 65-70.

14. L. Stryer, *J. Biol. Chem.*, 2012, **287**, 15164-15173.

15. L. Stryer, *J. Mol. Biol.*, 1965, **13**, 482-495.

16. D. I. Cattoni, S. B. Kaufman and F. L. G. Flecha, *Biochim. Biophys. Acta – Proteins Proteomics*, 2009, **1794**, 1700-1708.

17. G. Sudlow, D. J. Birkett and D. N. Wade, *Mol. Pharmacol.*, 1973, **9**, 649-657.

18. G. Sudlow, D. J. Birkett and D. N. Wade, *Mol. Pharmacol.*, 1975, **11**, 824-832.

19. G. Sudlow, D. J. Birkett and D. N. Wade, *Mol. Pharmacol.*, 1976, **12**, 1052-1061.

20. T. Peters Jr., *All about Albumin: Biochemistry, Genetics, and Medical Applications*, Academic Press, San Diego, CA, 1995.

21. G. E. Dobretsov, T. I. Syrejschikova, N. V. Smolina and M. G. Uzbekov, in *Human Serum Albumin (HSA): Functional Structure, Synthesis and Therapeutic Uses*, Nova Science Publishers, New York, NY, 2015, chapter 7, pp 129-171.

22. T. Peters Jr., *Adv. Protein Chem.*, 1985, **37**, 161-245.

23. S. Curry, *Vox Sang.*, 2002, **83**, 315-319.

24. R. Brodersen, T. Sjödin and I. Sjöholm, *J. Biol. Chem.*, 1977, **252**, 5067-5072.